Influence of Base Stacking and Hydrogen Bonding on the Fluorescence of 2-Aminopurine and Pyrrolocytosine in Nucleic Acids†

Samantha J. O. Hardman and Katherine C. Thompson*

School of Biological and Chemical Sciences, Birkbeck University of London, Malet Street, London WC1E 7HX, U.K.

Received March 10, 2006; Revised Manuscript Received June 2, 2006

ABSTRACT: Fluorescent nucleobase analogues are used extensively to probe the structure and dynamics of nucleic acids. The fluorescence of the adenine analogue 2-aminopurine and the cytosine analogue pyrrolocytosine is significantly quenched when the bases are located in regions of double-stranded nucleic acids. To allow more detailed structural information to be obtained from fluorescence studies using these bases, we have studied the excited-state properties of the bases at the CIS and TDB3LYP level in hydrogen-bonded and base-stacked complexes. The results reveal that the first excited state (the fluorescent state) of a hydrogen-bonded complex containing 2-aminopurine and thymine is just the first excited state of 2-aminopurine alone. However, the same cannot be said for structures in which 2-aminopurine is base stacked with other nucleobases. Stacking causes the molecular orbitals involved in the fluorescence transition to spread over more than one base. The predicted rate for the fluorescence transition is reduced, thus reducing the fluorescence quantum yield. The decrease in radiative rate varies with the stacking arrangement (e.g., A- or B-form DNA) and with the identity of the nucleobase with which 2-aminopurine is stacked. Stacking 2-aminopurine between two guanine moieties is shown to significantly decrease the energy gap between the first and second excited states. We do not find reliable evidence for a low-energy charge-transfer state in any of the systems that were studied. In the case of pyrrolocytosine, base stacking was found to reduce the oscillator strength for the fluorescence transition, but very little spreading of molecular orbitals across more than one base was observed.

Environment sensitive fluorescent analogues of the natural nucleobases are used extensively to study conformational changes of both RNA and DNA (*1*, *2*). The adenine analogue 2-aminopurine, shown in Figure 1, is a highly fluorescent isomer of adenine (6-aminopurine). The fluorescence excitation spectrum of 2-aminopurine has an excitation maximum at ∼305 nm, considerably red-shifted compared to those of the natural nucleobases, allowing 2-aminopurine to be selectively excited in the presence of the other bases. The substitution of 2-aminopurine for adenine in a nucleic acid causes little perturbation to the structure of a nucleic acid as, like adenine, 2-aminopurine will base pair with thymine in DNA or uracil in RNA. Experimental measurements reveal that the fluorescence of 2-aminopurine is strongly quenched when it is incorporated into a single strand of nucleic acid, and the fluorescence is quenched still further if the single strand of nucleic acid binds to a complementary strand and forms a helix (*1*, *2*). It is this sensitivity of the fluorescence of 2-aminopurine to its local environment that is exploited by experimentalists when they use the fluorescence of 2-aminopurine as a marker for local structure in nucleic acid studies. In this paper, we aim to understand the quenching mechanism of 2-aminopurine in a nucleic acid at the molecular level so that experimentally determined changes in the fluorescence properties of macromolecules containing 2-aminopurine (such as changes in fluorescence intensity and excited-state lifetime) can be used to elucidate much more detailed structural information.

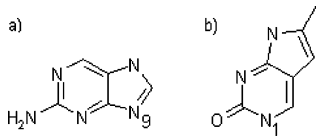

FIGURE 1: Structures of 2-aminopurine (a) and pyrrolocytosine (b). In a nucleic acid, 2-aminopurine would link to the sugar via the nitrogen labeled N_9 and pyrrolocytosine via the nitrogen labeled N_1.

Disagreement exists in the literature about the photophysical−photochemical mechanism that causes the fluorescence of 2-aminopurine to change with local structural changes such as helix formation, in particular whether charge transfer to or from a 2-aminopurine moiety in a nucleic acid occurs as a direct result of single-photon excitation at 305 nm (*3*−*11*). Although there have been numerous experimental studies on the fluorescence of 2-aminopurine in dinucleotides and small oligomers of DNA and RNA (*5*, *9*, *12*−*15*), a charge-separated product (e.g., $2AP^{\bullet-}$) has yet to be observed as a result of single-photon excitation at 305 nm (*3*). In contrast to this, calculations by Jean and Hall considerably strengthen the theory that fluorescence quenching of 2-aminopurine in nucleic acids occurs via a direct charge-transfer process (*16*, *17*). Jean and Hall calculated vertical transition energies (energies of the different electronic states of the molecule in the same geometry) and oscillator strengths associated with radiative transitions between the excited states and the ground

† This work was supported by The Royal Society (Grant 23699). S.J.O.H. thanks E Wood Limited for the award of a Dr. Kut scholarship.

10.1021/bi060479t CCC: $33.50
Published on Web 07/06/2006

state for proxies of di- and trinucleotides containing 2-aminopurine using time-dependent density functional theory (TDDFT)[1] with the B3LYP functional, TDB3LYP (*18*, *19*). The results suggested that when 2-aminopurine is stacked with other nucleobases low-lying charge-transfer states (dark states) are formed which have a major influence on the photophysics of 2-aminopurine and can lead to efficient fluorescence quenching of 2-aminopurine in base-stacked environments. In this work, we have examined the effects of both hydrogen bonding and base stacking on the fluorescence of 2-aminopurine using the configuration interaction singles (CIS) method (*20*) to better understand the mechanism(s) by which the fluorescence of 2-aminopurine is quenched in a helical environment. Calculations have also been performed using the TDB3LYP method to illustrate problems inherent in this method, specifically, the incorrect prediction by the TDB3LYP method of low-lying charge-transfer states in base-stacked systems.

2-Aminopurine is not the only nucleobase analogue to undergo fluorescence quenching in a helical environment. A complementary series of calculations have been carried out on the fluorescent cytosine analogue pyrrolocytosine (shown in Figure 1). The fluorescence of pyrrolocytosine is also quenched in doubled-stranded DNA compared to single-stranded DNA (*1*, *21*, *22*), but the results of calculations reported in this work suggest that the underlying mechanism may be quite different from that of 2-aminopurine.

METHODS

Geometries Used for Hydrogen-Bonded Complexes. The vertical transition energies to excited states of a complex in which 2-aminopurine is hydrogen-bonded to thymine were investigated. The structure of the 2-aminopurine·thymine base pair was obtained by mutating an adenine, from a Watson−Crick bonded adenine·thymine base pair, to 2-aminopurine. Two structures for the adenine·thymine base pair were used, one from an 11 bp structure of canonical A-form DNA [produced using Spartan02 (*23*)] and one from an 11 bp structure of canonical B-form DNA. In both cases, the DNA oligomers contained only adenine·thymine base pairs and the middle (sixth) base pair was selected for mutation to 2-aminopurine. The linking sugars and phosphates were removed and the bases terminated with hydrogens at the N_1 (pyrimidines) or N_9 (purines) position as appropriate. The thymine was replaced with the MP2/6-31G(d,p) optimized structure of thymine, and the adenine was replaced with an optimized structure of 2-aminopurine obtained with C_s symmetry imposed. Two different optimized structures of 2-aminopurine were used: one for the base in its ground-state (S_0) geometry, optimized at the MP2/6-31G(d,p) level, and one for the base in the geometry of its first excited state (S_1), a $\pi\pi^*$ state, optimized at the CIS/6-31G(d,p) level. In the case of the ground-state structure, a vibrational frequency analysis revealed one negative frequency associated with pyramidization of the external NH_2 unit; however, the C_s symmetry restriction was not removed as in a nucleic acid in aqueous solution flattening of external amino groups to give planar structures is expected. A frequency analysis of the optimized $\pi\pi^*$ excited-state structure revealed no negative frequencies, indicating that a true minimum energy structure had been found. The calculations on the structures in which the fluorescent base is in its ground-state geometry provide the predicted absorption wavelengths and oscillator strengths, whereas those in which the fluorescent base is in its first $\pi\pi^*$ excited-state geometry provide the expected wavelength and associated oscillator strength for the fluorescence transition.

Geometries Used for Base-Stacked Complexes. Oligomers (11 bp) of doubled-stranded $^{5'}$TTTTTATTTTT$^{3'}$, $^{5'}$CCCCCAC-CCCC$^{3'}$, $^{5'}$GGGGGAGGGGG$^{3'}$, and $^{5'}$AAAAAAAAAAA$^{3'}$ in both A- and B-form DNA were created using Spartan02. The sixth base in each oligomer was replaced with 2-aminopurine, and base-stacked structures of both A- and B-form $^{5'}$X2AP$^{3'}$, $^{5'}$2APX$^{3'}$, and $^{5'}$X2APX$^{3'}$, where X is cytosine, guanine, thymine, or adenine and 2AP is 2-aminopurine, were selected from the oligomers. As before, the phosphates and sugar units were removed and all bases terminated with hydrogens. The structures of the natural nucleobases were replaced with those obtained from optimizations at the MP2/6-31G(d,p) level with C_s symmetry imposed except in the case of thymine. As described above, two structures for 2-aminopurine were used, one for the base in its ground-state (S_0) geometry and one for the base in the geometry of its first excited state (S_1).

2-Aminopurine Nucleoside and Nucleotide. Computational resources do not at present allow for a complete quantum mechanical calculation of even small (di- and tri-) nucleotides containing both the sugar and phosphate linking groups. To ascertain the influence of the linking sugar and phosphate groups on the fluorescent properties of 2-aminopurine, the vertical transition energies of the 2-aminopurine deoxyriboside and deoxynucleotide were calculated. The structure of 2-aminopurine in both its ground-state and first excited-state geometry was used, and the sugar and phosphate groups were in the geometry they would have in canonical A- and B-form DNA.

Pyrrolocytosine Complexes. In addition to these calculations involving 2-aminopurine, calculations in which pyrrolocytosine is base-stacked with guanine were also carried out. Pyrrolocytosine (PC) was arranged with guanine stacked above and below it, $^{5'}$GPCG$^{3'}$, as it would be arranged in A-form DNA (2.548 Å rise per base, 32.70° twist) and B-form DNA (3.375 Å rise per base, 36.00° twist). Two different geometries were used, one for the base in its ground-state (S_0) geometry, optimized at the MP2/6-31G(d,p) level with C_s symmetry, and one for the base in the geometry of its first excited state (S_1), a nonplanar $\pi\pi^*$ state (*24*), optimized at the CIS/6-31+G(d,p) level with no symmetry constraints imposed.

All structures for which results are presented in this work have been made available as part of the Supporting Information.

Computational Methods. The first 10 vertical transition energies were calculated for all structures considered in this work at the CIS/6-31+G(d,p) level. In the case of the 2-aminopurine hydrogen-bonded or base-stacked with thymine, and the structures involving pyrrolocytosine, the vertical transition energies predicted using the TDB3LYP/

[1] Abbreviations: TDDFT, time-dependent density functional theory; TDB3LYP, time-dependent density functional theory with the B3LYP hybrid functional; CIS, configuration interaction singles; 2AP, 2-aminopurine; PC, pyrrolocytosine; 2APdr, 2-aminopurine deoxyriboside; 2APdrp, 2-aminopurine deoxynucleotide.

Table 1: Wavelengths and Oscillator Strengths, *f*, Calculated at the CIS/6-31+G(d,p) Level for the First (lowest-energy) Transition of 2-Aminopurine (2AP) Alone and 2-Aminopurine Hydrogen-Bonded to Thymine (T)

	2AP in ground-state geometry (relevant to absorption process)			2AP in excited-state geometry (relevant to fluorescence process)		
structure	λ^a (nm)	*f*	assignment	λ^a (nm)	*f*	assignment
2AP alone	315	0.334	$\pi_{2AP}\pi^*_{2AP}$	342	0.371	$\pi_{2AP}\pi^*_{2AP}$
2AP-T H-bonding, A-form DNA	320	0.364	$\pi_{2AP}\pi^*_{2AP}$	346	0.409	$\pi_{2AP}\pi^*_{2AP}$
2AP-T H-bonding, B-form DNA	320	0.363	$\pi_{2AP}\pi^*_{2AP}$	345	0.408	$\pi_{2AP}\pi^*_{2AP}$

[a] All energies have been scaled by a factor of 0.72.

6-31+G(d,p) method were also calculated. In our previous paper (*24*), we examined the influence of the basis set on the predicted transitions. We concluded that there was no significant benefit in using the 6-311G (or cc-pVTZ) basis set over the smaller 6-31G (or cc-pVDZ) basis set; however, the inclusion of diffuse functions was necessary as not only did the absolute energy and spacing between excited states prove to be sensitive to the inclusion of diffuse functions but failure to include diffuse functions resulted in the prediction of no low-lying Rydberg states. It is known that low-lying Rydberg states play an important role in many photochemical reactions and therefore should not be ignored (*25*). What we did not examine in our previous work was whether it was necessary to include diffuse functions on both hydrogen and heavy atoms, or if equally good results could be obtained with the inclusion of diffuse functions on heavy atoms only, for example, if the slightly smaller basis set, 6-31+G(d,p), could be used instead of the 6-31++G(d,p) basis set. We have therefore performed calculations at both the CIS/6-31++G(d,p) and CIS/6-31+G(d,p) levels on structures in which pyrrolocytosine is sandwiched between two guanine molecules, as it would be in DNA.

All electronic structure calculations were performed using the Gaussian 03 suite of programs (*26*). The molecular orbitals were viewed using either Molekel (*27*) or Chemcraft (*28*).

RESULTS

Hydrogen Bonding in 2-Aminopurine. Table 1 shows the transition energies and oscillator strengths predicted at the CIS/6-31+G(d,p) level for the complex in which 2-aminopurine is hydrogen-bonded to thymine. The energies of $\pi\pi^*$ states predicted by the CIS method are known to be too large, and thus, all energies based on CIS calculations reported in this work have been scaled by a constant factor of 0.72, as recommended by Broo and Holmén (*29*). The absolute values of the oscillator strengths predicted by the CIS method are also too large, but as the discussion focuses on the relative changes in the values of the oscillator strengths, rather than the absolute values, no correction has been applied. Wavelengths of the scaled absorbance and fluorescence maxima, 315 and 342 nm, are in good agreement with the values of Rachofsky et al. (*30*), 312 and 338 nm, respectively, obtained using the much higher level method, complete active space self-consistent field (CASSCF) supplemented using multiconfigurational quasi-degenerate perturbation theory (MCQDPT). The results presented in this work are for the molecules in vacuo; the measured absorbance and fluorescence maxima of 2-aminopurine in aqueous solution are ~305 and 370 nm, respectively (*1*).

The CIS method predicts that the first excited state for complexes of 2-aminopurine hydrogen-bonded to thymine

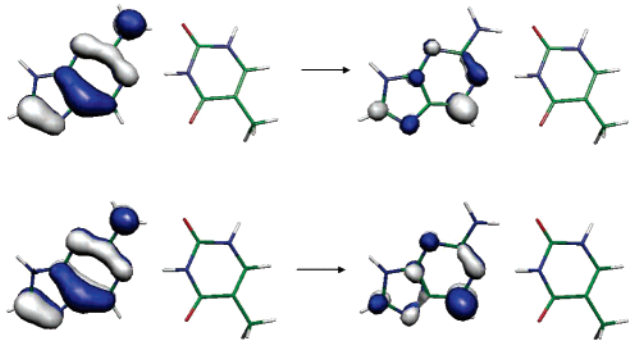

FIGURE 2: Orbitals involved in the first transition of the complex in which 2-aminopurine is hydrogen-bonded to thymine, as predicted by the CIS method. In the top diagram, 2-aminopurine is in its optimized ground-state geometry, while in the bottom diagram, 2-aminopurine is in the optimized geometry of its first excited state (a $\pi\pi^*$ state).

is of $\pi\pi^*$ character and the orbitals involved in the fluorescence transition (shown in Figure 2) are centered solely on 2-aminopurine and resemble those involved in the first transition of 2-aminopurine itself. The wavelength is slightly, ~4 nm, red shifted compared to that of free 2-aminopurine, and the oscillator strength for the transition from the ground state to this excited state is greater, by ~10%, than that of the analogous transition of 2-aminopurine alone. These results are slightly different from those reported previously for pyrrolocytosine (*24*). In the case of pyrrolocytosine, although a red shift was also calculated for the fluorescence transition upon hydrogen bonding (to guanine), the associated oscillator strength was no larger than that for the fluorescence transition pyrrolocytosine alone.

The results from the TDB3LYP method, shown in Table 2, are very different from those obtained using the CIS method. For the free base, the wavelength predicted for the first transition, to a $\pi\pi^*$ state, is 290 nm and the oscillator strength for this transition is 0.131. However, when 2-aminopurine is hydrogen-bonded to thymine, the wavelength for the first transition is ~317 nm and the oscillator strength is extremely small, ~0.002. The reason for this dramatic change is that the first excited state predicted by the TDB3LYP method for the hydrogen-bonded complex is of charge-transfer character: an electron is promoted from a π orbital centered on 2-aminopurine into a vacant π^* orbital of thymine, and the orbitals that are involved are shown in Figure 3. However, it is known that although local and hybrid TDDFT methods such as TDB3LYP can be used to predict accurate energies and transition dipole moments for valence states (such as local $\pi\pi^*$ states), the methods seriously underestimate the energies of charge-transfer states; the reasons for this are fully discussed in the review by Dreuw and Head-Gordon (*31*) and references therein but are briefly

Table 2: Wavelengths and Oscillator Strengths (*f*) Calculated at the TDB3LYP/6-31+G(d,p) Level for the First and Second Transitions of 2-Aminopurine (2AP) Alone and 2-Aminopurine Hydrogen-Bonded to Thymine (T)[a]

	first transition			second transition		
structure	λ (nm)	*f*	assignment	λ (nm)	*f*	assignment
2AP alone	290	0.131	$\pi_{2AP}\pi^*_{2AP}$	276	0.002	$n_{2AP}\pi^*_{2AP}$
2AP-T H-bonding, A-form DNA	319	0.002	$\pi_{2AP}\pi^*_{T}$	304	0.130	$\pi_{2AP}\pi^*_{2AP}$
2AP-T H-bonding, B-form DNA	316	0.003	$\pi_{2AP}\pi^*_{T}$	303	0.130	$\pi_{2AP}\pi^*_{2AP}$

[a] Both bases are in the optimized geometries of their ground states.

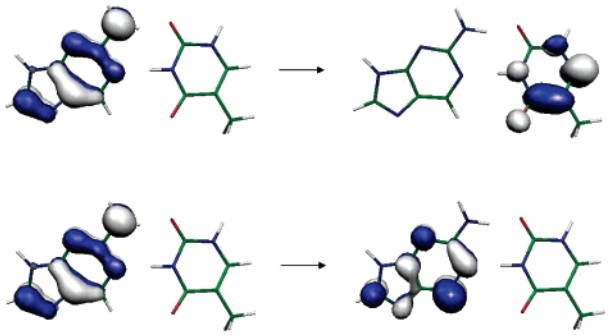

FIGURE 3: Orbitals involved in the first transition (top pair) and second transition (bottom pair) of the complex in which 2-aminopurine, in its ground-state geometry, is hydrogen-bonded to thymine, as predicted by the TDB3LYP method. The first transition is erroneously predicted to be of charge-transfer character.

relayed here. Charge-transfer states should be characterized by a long-range Coulombic potential (the attraction between molecule A, which is left with a positive charge, and molecule B, which is left with a negative charge). As this stabilizing Coulombic interaction falls off with $1/R$ (where R is the separation between molecules A and B), the energy of the charge-transfer state should increase with $1/R$. The energy of charge-transfer states computed using the TDB3LYP method increases only with $0.2/R$ because the functional does not exhibit the appropriate long-range behavior. If the long-range behavior of the functional is corrected, then the situation is greatly improved. For example, Kobayashi and Amos (*32*) showed that, in contrast to experimental results (*33*), TDB3LYP theory predicts two low-lying charge-transfer states for the phenylene-linked zincbacteriochlorin−bacteriochlorin complex (ZnBC−BC) 0.45 and 0.29 eV below the first valence transition (a $\pi\pi^*$ transition on ZnBC). The use of the long-range corrected functional (CAM-B3LYP) corrects the ordering of excited states: the charge-transfer states are now predicted to be ~1 eV above the valence $\pi\pi^*$ transitions of both ZnBC and BC. In summary, although valence states are generally very well described using the TDB3LYP (more accurately so than the CIS method that systematically overpredicts excitation energies and hence the excitation energies predicted require scaling), the TDB3LYP method grossly underpredicts the energies of charge-transfer states. Thus, the prediction of low-lying charge-transfer states by the TDB3LYP method should be treated with extreme caution.

In the case of 2-aminopurine hydrogen-bonded to thymine, the second transition predicted by the TDB3LYP method is of $\pi\pi^*$ character and the orbitals that are involved are the same orbitals as those involved in the first transition of 2-aminopurine alone. The wavelength of this second transition is red-shifted compared to that of 2-aminopurine alone, but the oscillator strength is virtually unchanged. Thus, if the spurious charge-transfer state is ignored, the TDB3LYP method predicts that hydrogen bonding to thymine will red shift the absorption maximum of 2-aminopurine by ~13 nm but scarcely affect the oscillator strength for the transition.

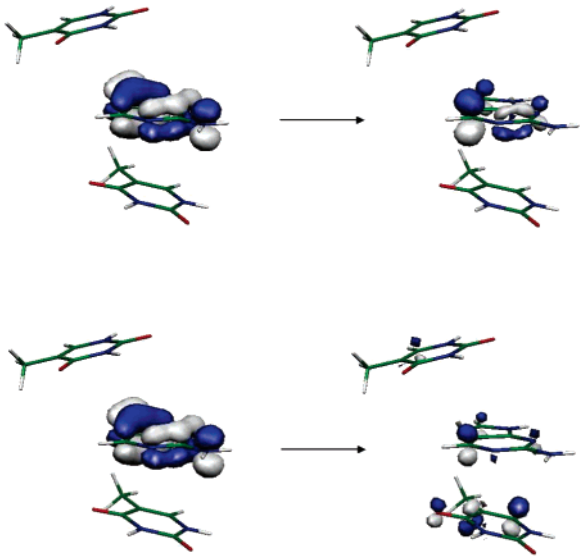

FIGURE 4: Orbitals involved in the first transition of a complex in which 2-aminopurine is stacked between two thymines as it would be in A-form DNA. The transition is of $\pi\pi^*$ character, and the main contribution to the transition is made by the top pair of orbitals which are located solely on the 2-aminopurine moiety. However, a significant contribution to the transition is made by the lower pair of orbitals in which the π^* orbital has a component on each of the three bases, with the ^{3}′T having the largest component. 2-Aminopurine is in the optimized geometry of its first excited state.

Base Stacking in 2-Aminopurine. Table 3 shows the results obtained at the CIS/6-31+G(d,p) level for complexes in which 2-aminopurine is stacked with a nucleobase above and/or below it as it would be in doubled-stranded DNA. When 2-aminopurine is stacked with one or more nucleobases, the wavelength for the absorption is shifted slightly (−1 to 7 nm red-shifted), the extent depending upon both the identity of the base and the type of stacking (A- or B-form). In all cases, the first transition is of $\pi\pi^*$ character; however, although π and π^* orbitals of 2-aminopurine are always involved, orbitals with coefficients on more than one base are frequently involved. In the case of stacking with thymine [the natural nucleobase with the highest electron affinity (*34*)] or cytosine, a contribution to the fluorescence transition is made from promotion of an electron to a π^* orbital that is spread over one or more of the other bases, as illustrated in Figure 4. In the case of stacking with guanine [the most readily oxidized natural nucleobase (*34*)], the transition often involves the promotion of an electron from a π orbital spread over both 2-aminopurine and guanine, illustrated in Figure

Table 3: Wavelengths and Oscillator Strengths (*f*) Calculated at the CIS/6-31+G(d,p) Level for the First (lowest-energy) Transition of Base-Stacked Structures (givens in the order from 5′ to 3′) Containing 2-Aminopurine (2AP) Stacked with Thymine (T), Cytosine (C), Adenine (A), or Guanine (G)

	2AP in ground-state geometry (relevant to absorption process)			2AP in excited-state geometry (relevant to fluorescence process)		
structure	λ^a (nm)	*f*	assignment	λ^a (nm)	*f*	assignment
2AP alone	315	0.334	$\pi_{2AP}\pi^*_{2AP}$	342	0.371	$\pi_{2AP}\pi^*_{2AP}$
2AP stacked with thymine						
2APT, A-form	316	0.274	$\pi_{2AP}\pi^*_{2AP}{}^b$	343	0.306	$\pi_{2AP}\pi^*_{2AP}{}^b$
T2AP, A-form	314	0.249	$\pi_{2AP}\pi^*_{2AP}{}^b$	341	0.297	$\pi_{2AP}\pi^*_{2AP}{}^b$
T2APT, A-form	314	0.204	$\pi_{2AP}\pi^*_{5'T,2AP,T3'}$	341	0.246	$\pi_{2AP}\pi^*_{2AP}{}^c$
2APT, B-form	317	0.285	$\pi_{2AP}\pi^*_{2AP,T}$	345	0.318	$\pi_{2AP}\pi^*_{2AP,T}$
T2AP, B-form	316	0.240	$\pi_{2AP}\pi^*_{2AP}$	343	0.288	$\pi_{2AP}\pi^*_{2AP}{}^b$
T2APT, B-form	318	0.205	$\pi_{2AP}\pi^*_{5'T,2AP,T3'}$	345	0.249	$\pi_{2AP}\pi^*_{2AP}{}^c$
2AP stacked with cytosine						
2APC, A-form	318	0.257	$\pi_{2AP}\pi^*_{2AP,C}$	345	0.302	$\pi_{2AP}\pi^*_{2AP,C}$
C2AP, A-form	318	0.266	$\pi_{2AP}\pi^*_{C,2AP}$	345	0.306	$\pi_{2AP}\pi^*_{2AP,C}$
C2APC, A-form	320	0.207	$\pi_{2AP}\pi^*_{2AP}{}^b$	348	0.252	$\pi_{2AP}\pi^*_{5'C,2AP,3'C}$
2APC, B-form	319	0.289	$\pi_{2AP}\pi^*_{2AP,C}$	347	0.321	$\pi_{2AP}\pi^*_{2AP,C}$
C2AP, B-form	317	0.249	$\pi_{2AP}\pi^*_{C,2AP}$	344	0.294	$\pi_{2AP}\pi^*_{C,2AP}$
C2APC, B-form	321	0.222	$\pi_{2AP}\pi^*_{5'C,2AP,C3'}$	349	0.260	$\pi_{2AP}\pi^*_{5'C,2AP,C3'}$
2AP stacked with adenine						
2APA, A-form	319	0.217	$\pi_{2AP}{}^b\pi^*_{2AP}{}^b$	346	0.274	$\pi_{2AP}\pi^*_{2AP}{}^b$
A2AP, A-form	317	0.208	$\pi_{2AP}\pi^*_{2AP}{}^b$	344	0.254	$\pi_{2AP}\pi^*_{2AP}{}^b$
A2APA, A-form	320	0.135	$\pi_{2AP}{}^b\pi^*_{2AP}{}^b$	347	0.189	$\pi_{2AP}\pi^*_{2AP}{}^b$
2APA, B-form	318	0.208	$\pi_{2AP}\pi^*_{2AP}{}^b$	346	0.257	$\pi_{2AP}\pi^*_{2AP}{}^b$
A2AP, B-form	319	0.215	$\pi_{2AP}{}^b\pi^*_{2AP}$	346	0.257	$\pi_{2AP}\pi^*_{2AP}$
A2APA, B-form	321	0.134	$\pi_{2AP}\pi^*_{2AP}{}^b$	349	0.178	$\pi_{2AP}\pi^*_{2AP}$
2AP stacked with guanine						
2APG, A-form	317	0.231	$\pi_{2AP}{}^b\pi^*_{2AP}$	343	0.282	$\pi_{2AP}\pi^*_{2AP}$
G2AP, A-form	313	0.206	$\pi_{2AP}\pi^*_{2AP}$	340	0.256	$\pi_{2AP}{}^b\pi^*_{2AP}$
G2APG, A-form	314	0.139	$\pi_{5'G,2AP,G3'}\pi^*_{2AP}$	341	0.194	$\pi_{2AP}\pi^*_{2AP}$
2APG, B-form	318	0.207	$\pi_{2AP}\pi^*_{2AP}$	345	0.260	$\pi_{2AP}\pi^*_{2AP}$
G2AP, B-form	315	0.204	$\pi_{2AP}\pi^*_{2AP}$	342	0.254	$\pi_{2AP}{}^b\pi^*_{2AP}$
G2APG, B-form	317	0.121	$\pi_{5'G,2AP,G3'}\pi^*_{2AP}$	344	0.176	$\pi_{2AP}{}^b\pi^*_{2AP}$

[a] All energies have been scaled by a factor of 0.72. [b] The main contribution to the transition is from an orbital mainly centered on 2-aminopurine, but a small contribution is made from an orbital(s) spread over 2-aminopurine and one of the other bases only. [c] The main contribution to the transition is from an orbital centered on 2-aminopurine, but a small contribution is made from orbital(s) spread over all bases.

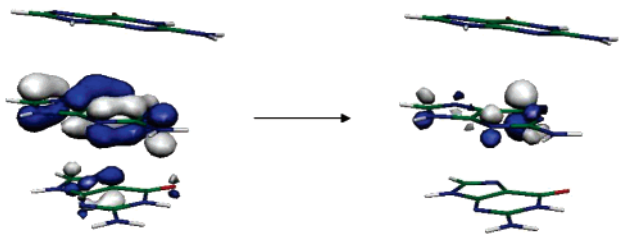

FIGURE 5: Orbitals which make the largest contribution to the first transition of a complex in which 2-aminopurine is stacked between two guanines, as it would be in B-form DNA. The transition is of $\pi\pi^*$ character, but the π orbital is located on both the 5′G and the 2AP moiety. 2-Aminopurine is in the optimized geometry of its first excited state.

5.[2] In the case of adenine, when 2-aminopurine is in its ground-state geometry both the π and the π^* orbitals involved in the first $\pi\pi^*$ transition are often found to have coefficients on both 2-aminopurine and one or both of the adenines. In summary, calculations at the CIS level reveal that the transitions between the ground and first excited state of structures in which 2-aminopurine is base stacked with one or more other bases, as it would be in DNA, are not simply the sum of transitions of 2-aminopuurine alone and transitions of the other nucleobases alone. The orbitals that are involved in the first (lowest-energy) transition are of the π type in all cases, but a contribution (often the major contribution) is made from transition between orbitals with coefficients on more than one base, rather than localized on one specific base. The change in orbitals that are involved is associated with a large change in the oscillator strength for the first $\pi\pi^*$ transitions. When one pyrimidine base, cytosine or thymine, is stacked above or below 2-aminopurine, the oscillator strength for the absorption process is decreased by 13−28% and that of the fluorescence process by 13−21%. When 2-aminopurine is sandwiched between two pyrimidine bases, the oscillator strengths are reduced by 33−39 and 30−34% for the absorption and fluorescence processes, respectively. Stacking a purine base, adenine or guanine, above or below 2-aminopurine results in a larger reduction in oscillator strength for the $\pi\pi^*$ transition: 31−39% reduction for the absorption process and 24−32% reduction for the fluorescence process. Sandwiching 2-aminopurine between two purine bases reduces the oscillator strength for the absorption process by 58−64% and that of the fluorescence process by 48−53%. Thus, unlike hydrogen bonding, base stacking is predicted to significantly reduce the oscillator strength for both the absorption process (and hence the absorption coefficient) and the fluorescence process (and hence the radiative rate). This result is in agreement with the experimental work of Rachofsky et al. (*36*), who reported that base pairing does not cause fluorescence

[2] The spreading of molecular orbitals across more than one nucleobase in base-stacked structures is well-known; for instance, when two guanine moieties are adjacent in a base-stacked environment, the HOMO, although mainly on the 5′-guanine, has a component on both bases and is lower in energy than the HOMO of a free guanine (*35*).

Table 4: Wavelengths and Oscillator Strengths (*f*) Calculated at the TDB3LYP/6-31+G(d,p) Level for the First and Second Transitions of 2-Aminopurine (2AP) Base-Stacked with Thymine (T)[a]

	first transition			second transition		
structure	λ (nm)	*f*	assignment	λ (nm)	*f*	assignment
2AP alone	290	0.131	$\pi_{2AP}\pi^*_{2AP}$	276	0.002	$n_{2AP}\pi^*_{2AP}$
T2AP, A-form	303	0.003	$\pi_{2AP}\pi^*_{T}$	290	0.110	$\pi_{2AP}{}^b\pi^*_{2AP}{}^b$
2APT, A-form	310	0.011	$\pi_{2AP}{}^b\pi^*_{2AP,T}$	296	0.091	$\pi_{2AP}{}^b\pi^*_{2AP,T}$
T2AP, B-form	302	0.001	$\pi_{2AP}\pi^*_{T}$	292	0.103	$\pi_{2AP}\pi^*_{2AP}$
2APT, B-form	328	0.001	$\pi_{2AP}\pi^*_{T}$	294	0.107	$\pi_{2AP}\pi^*_{2AP}$

[a] Both bases are in the optimized geometries of their ground states. [b] The main contribution to the transition is from an orbital mainly centered on 2-aminopurine, but a small contribution is made from an orbital(s) spread over both 2-aminopurine and thymine.

Table 5: Wavelengths and Oscillator Strengths (*f*) Calculated at the CIS/6-31+G(d,p) Level for the First Transition of 2-Aminopurine Deoxyriboside (2APdr) and 2-Aminopurine Nucleotide (2APdrp)

	2AP in ground-state geometry (relevant to absorption process)			2AP in excited-state geometry (relevant to fluorescence process)		
structure	λ^a (nm)	*f*	assignment	λ^a (nm)	*f*	assignment
2AP alone	315	0.334	$\pi_{2AP}\pi^*_{2AP}$	342	0.371	$\pi_{2AP}\pi^*_{2AP}$
2APdr, A-form	315	0.391	$\pi_{2AP}\pi^*_{2AP}$	343	0.430	$\pi_{2AP}\pi^*_{2AP}$
2APdr, B-form	316	0.387	$\pi_{2AP}\pi^*_{2AP}$	343	0.424	$\pi_{2AP}\pi^*_{2AP}$
2APdrp, A-form	319	0.359	$\pi_{2AP}\pi^*_{2AP}$	348	0.399	$\pi_{2AP}\pi^*_{2AP}$
2APdrp, B-form	318	0.362	$\pi_{2AP}\pi^*_{2AP}$	346	0.400	$\pi_{2AP}\pi^*_{2AP}$

[a] All energies have been scaled by a factor of 0.72.

quenching of 2-aminopurine whereas base stacking does. The results indicate that the degree to which the oscillator strength for the fluorescence transition is suppressed by base stacking depends both on the identity of the base with which 2-aminopurine is stacked (purines always reduce the oscillator strength more than pyrimidines) and on the orientation of the bases above and below 2-aminopurine. For instance, when 2-aminopurine is sandwiched between two cytosines as it would be in A-form DNA, the reduction in the oscillator strength (38%) is greater than when 2-aminopurine is stacked between two cytosines as it would be in B-form DNA (33%). The converse is found in the case of stacking with guanine: a much larger reduction in the oscillator strength (64%) for the B-form structure $^{5'}$G2APG$^{3'}$ than for the A-form structure (58%). In the case of stacking with thymine or adenine, although the oscillator strength is reduced by base stacking, the reduction is insensitive to the nature of the stacking.

The results obtained at the TDB3LYP/6-31+G(d,p) level for complexes in which 2-aminopurine is stacked with thymine above and/or below it as it would be in doubled-stranded DNA are shown in Table 4. In general, the method predicts that the first transition is of charge-transfer character while the second transition is a localized transition involving orbitals of 2-aminopurine only. The exception is the $^{3'}$2APT$^{5'}$ structure obtained from A-form DNA; in this case, both the π and π^* orbitals involved in the first and second transition are spread over both bases. The results of the TDB3LYP calculations agree well with those obtained by Jean and Hall (*17*), who carried out similar calculations and reported the existence of low-lying charge-transfer states in base-stacked systems containing 2-aminopurine. However, as we have said above, the low-lying charge-transfer states predicted by the TDB3LYP method are merely an artifact of the method and should be disregarded.

The second transition for structures in which 2-aminopurine is stacked with thymine is predicted by the TDB3LYP method to be very similar to the first transition of 2-aminopurine alone, involving the same orbitals (except for the $^{3'}$2APT$^{5'}$ structure, as mentioned above) and occurring at a similar wavelength, ~290 nm. In agreement with the CIS calculations, a significant reduction in the oscillator strength is predicted for this transition to the S_2 $\pi\pi^*$ state, compared to the analogous transition of the free base.

2-Aminopurine Nucleoside and Nucleotide. The results of the CIS calculations on nucleosides and nucleotides containing 2-aminopurine (Table 5) confirm that the sugar and the phosphate groups have only a very slight effect on the calculated absorption and fluorescence properties of 2-aminopurine. The lowest-energy excited state predicted in each case was the fluorescent $\pi\pi^*$ state located on the 2-aminopurine residue only. The addition of the sugar moiety red-shifts the predicted absorption and fluorescence wavelengths very slightly. The oscillator strength for the fluorescent transition is increased by ~15% via the addition of the sugar, but the addition of the phosphate group to the nucleoside reduces the oscillator strength for the fluorescence transition to just 8% larger than that for free 2-aminopurine itself.

Pyrrolocytosine. The results obtained at the CIS/6-31+G(d,p) level when pyrrolocytosine is stacked between two guanine units are given in Table 6, and results obtained at the TDB3LYP level are given in Table 7. Again, the TDB3LYP method erroneously predicts low-lying states in which an electron has been promoted from an orbital located on one base into an orbital centered purely on another base, although in this case the low-lying charge-transfer states predicted are higher in energy than the first, fluorescent, transition. The CIS method predicts that base stacking will significantly reduce the oscillator strength for the $\pi\pi^*$ transition; however, no spreading of the molecular orbitals involved across more than one base is observed, and the first transition in all cases involves a transition from an orbital located almost exclusively on pyrrolocytosine to another orbital located almost exclusively on pyrrolocytosine. The reductions in the oscillator strengths are slightly smaller than those encountered for 2-aminopurine. Stacking 2-aminopurine between two guanines resulted in an ~60% reduction in the oscillator strength for the absorption transition and an ~50% reduction in the oscillator strength for the fluorescence transition; in the case of pyrrolocytosine, the reductions are ~43 and 38%, respectively.

Tables 5 and 6 show the results obtained when the same system was studied at both the CIS/6-31+G(d,p) and the CIS/6-31++G(d,p) levels. It can be seen that both basis sets give essentially the same results. In both cases, the first transition is predicted to be of $\pi\pi^*$ character and is localized almost entirely on the pyrrolocytosine unit. The energy and oscillator strength for this transition are insensitive to the addition of diffuse functions to hydrogens as well as heavy atoms [i.e., in going from 6-31+G(d,p) to 6-31++G(d,p)]. Both basis sets predict the existence of relatively low-lying Rydberg states that are not predicted when the 6-31G(d,p) basis set is used (*24*). The oscillator strengths associated with transitions to these Rydberg states are not sensitive to the

Table 6: Wavelengths and Oscillator Strengths (*f*) Calculated at the CIS/6-31+G(d,p) Level for the First Transition of Pyrrolocytosine (PC) Alone and Stacked between Two Guanine (G) Molecules, As It Would Be in DNA[a]

	CIS/6-31+G(d,p)			CIS/6-31++G(d,p)		
structure	λ^b (nm)	*f*	assignment	λ^b (nm)	*f*	assignment
PC in ground-state geometry						
PC alone						
first transition	359	0.279	$\pi_{PC}\pi^*_{PC}$	358	0.279	$\pi_{PC}\pi^*_{PC}$
second transition	314	0.001		329	0.001	
third transition	291	0.003		302	0.002	
G-PC-G, A-form						
first transition	377	0.144	$\pi_{PC}\pi^*_{PC}$	377	0.145	$\pi_{PC}\pi^*_{PC}$
second transition	342	0.001		356	0.001	
third transition	308	0.004		322	0.004	
G-PC-G, B-form						
first transition	365	0.176	$\pi_{PC}\pi^*_{PC}$	365	0.172	$\pi_{PC}\pi^*_{PC}$
second transition	325	0.005		339	0.009	
third transition	297	0.010		309	0.006	
PC in excited-state geometry						
PC alone						
first transition	415	0.259	$\pi_{PC}\pi^*_{PC}$	416	0.256	$\pi_{PC}\pi^*_{PC}$
second transition	339	0.008		357	0.009	
third transition	312	0.003		327	0.002	
G-PC-G, A-form						
first transition	443	0.147	$\pi_{PC}\pi^*_{PC}$	443	0.146	$\pi_{PC}\pi^*_{PC}$
second transition	377	0.001		395	0.001	
third transition	336	0.008		352	0.006	
G-PC-G, B-form						
first transition	423	0.176	$\pi_{PC}\pi^*_{PC}$	424	0.174	$\pi_{PC}\pi^*_{PC}$
second transition	356	0.005		371	0.007	
third transition	321	0.005		335	0.005	

[a] Only valence transitions have been assigned. [b] All energies have been scaled by a factor of 0.72.

Table 7: Wavelengths and Oscillator Strengths (*f*) Calculated at the TDB3LYP/6-31+G(d,p) Level for the First and Second Transitions of Pyrrolocytosine (PC) Base-Stacked with Guanine (G)

	first transition			second transition		
structure	λ (nm)	*f*	assignment	λ (nm)	*f*	assignment
PC in ground-state geometry						
PC alone	352	0.073	$\pi_{PC}\pi^*_{PC}$	284	0.000	$n_{PC}\pi^*_{PC}$
G-PC-G, A-form	376	0.031	$\pi_{PC}\pi^*_{PC}$	318	0.003	$\pi_{PC}\pi^*_{5'G}$
G-PC-G, B-form	359	0.037	$\pi_{PC}\pi^*_{PC}$	332	0.004	$\pi_{5'G,3'G}\pi^*_{PC}$
PC in excited-state geometry						
PC alone	406	0.072	$\pi_{PC}\pi^*_{PC}$	299	0.001	$n_{PC}\pi^*_{PC}$
G-PC-G, A-form	446	0.032	$\pi_{PC}\pi^*_{PC}$	352	0.005	$\pi_{PC}\pi^*_{5'G}$
G-PC-G, B-form	420	0.040	$\pi_{PC}\pi^*_{PC}$	357	0.004	$\pi_{5'G}\pi^*_{PC}$

presence of the additional diffuse orbitals on hydrogen; however, it should be noted that the energy of the Rydberg states is reduced (by 0.14−0.19 eV) when the additional diffuse functions are added.

DISCUSSION

Comparison of the results obtained at the CIS and TDB3LYP levels, and reference to the literature, show that the low-lying charge-transfer states predicted by the TDB3LYP method, and used to explain the quenching of 2-aminopurine in a base-stacked environment, are not physically meaningful. The CIS method does not predict any low-lying charge-transfer states but does predict that the oscillator strength for the transition from the fluorescent $\pi\pi^*$ state (predicted to be the first excited state in all cases by the CIS methods) is decreased significantly when the fluorescent base 2-aminopurine is involved in a π-stacked environment, but not when 2-aminopurine is involved in hydrogen bonding alone. The oscillator strength, *f*, can be directly related to the rate constant for the fluorescence process, k_F, by eqs I and II (*37*):

$$k_F = \frac{1}{4\pi\epsilon_0}\frac{64\pi^4 n\langle\nu^{-3}\rangle^{-1}}{3hc^3}D \qquad \text{(I)}$$

where ϵ_0 is the permittivity of free space, n is the refractive index of the medium, ν is the frequency of the fluorescence transition ($\langle\nu^{-3}\rangle$ is the expectation value of ν^{-3}), h is Planck's constant, c is the speed of light in a vacuum, and D is the square of the transition dipole moment. The transition dipole moment is related to the oscillator strength, *f*, by eq II (*38*):

$$D = \frac{3he^2}{8\pi^2 m_e}\frac{f}{\nu} \qquad \text{(II)}$$

where e is the charge on an electron and m_e is the mass of an electron. As fluorescence is in competition with other, nonradiative processes, with a total rate coefficient of k_{NR}:

$$2AP^* \xrightarrow{k_F} 2AP + h\nu \quad (1)$$

$$2AP^* \xrightarrow{k_{NR}} 2AP \quad (2)$$

a reduction in oscillator strength would therefore lead to a decrease in the value of k_F and a reduction in the fluorescence quantum yield (ϕ_F):

$$\phi_F = \frac{k_F}{k_F + k_{NR}} \quad \text{(III)}$$

Thus, the CIS method, by predicting a lowering in the value of the oscillator strength for the fluorescence transition upon base stacking, does predict a reduction in the fluorescence quantum yield. The fluorescence quantum yield of isolated 2-aminopurine in neutral aqueous solutions at room temperature is ~0.66, and the quantum yield of the 2-aminopurine riboside is almost identical, 0.65−0.68 (*39*, *40*). The CIS method predicts that the oscillator strength for the fluorescence transition of 2-aminopurine alone is 0.371, but only ~0.282−0.260 for 2-aminopurine base-stacked with guanine, $^{5'}$2APG$^{3'}$. If the nonradiative processes were unchanged by base stacking (k_{NR} is unchanged), then the fluorescence quantum yield, calculated using eq III, would be 0.60−0.58, considerably larger than the experimental data suggest[3] (*5*, *12*). In addition to this, a decrease in the value of k_F, as predicted by the CIS calculations, would lead to an increase in the lifetime of the excited state, τ:

$$\tau = \frac{1}{k_F + k_{NR}} \quad \text{(IV)}$$

and this has not been observed experimentally. Experimental determinations of the lifetime of the excited fluorescent state of free 2-aminopurine vary between 2 and 12 ns (*5*, *13*, *40*−*42*) with more recent values lying between 9 and 12 ns (*5*, *13*, *40*, *41*). Using the values of Holmén et al. (*40*), a quantum yield of 0.66 and a τ of 11.8 ns, k_F is found to be 5.6×10^7 s^{-1} and k_{NR} to be 2.9×10^7 s^{-1}. The reduction in oscillator strength predicted for the fluorescence transition of the base-stacked system $^{5'}$2APG$^{3'}$ compared to that of free 2-aminopurine would lead to an increase in the excited-state lifetime from 11.8 to ~14−15 ns, if the nonradiative rate remained unchanged by base stacking. The experiments performed on dinucleotides and nucleic acid oligomers containing 2-aminopurine reveal that for each dinucleotide or oligomer the excited fluorescent state has several different lifetimes, presumably depending upon the local environment (e.g., degree of base stacking) of 2-aminopurine in the complex. All the lifetimes are, however, significantly shorter than that of free 2-aminopurine or 2-aminopurine riboside. Somsen et al. (*5*) have reported that for dinucelotides containing 2-aminopurine one excited fluorescent-state lifetime for each dinucleotide studied is similar to that of free 2-aminopurine; e.g., for the $^{5'}$2APG$^{3'}$ dinucleotide, the longest lifetime measured was 8.5 ns, but this lifetime is still slightly shorter than that of 2-aminopurine alone, rather than slightly longer. In summary, although the CIS calculations predict a reduction in the oscillator strength for the fluorescent transition, and hence a reduction in the fluorescence quantum yield when 2-aminopurine is involved in a base-stacked complex, the experimentally observed reduction in quantum yield and decrease in the excited-state lifetime can only be explained if an increase in the nonradiative rate accompanies the reduction in the fluorescence rate. A possible explanation for the change in the nonradiative rate with base stacking is that base stacking either changes the potential energy surface of the fluorescent S_1 state so that efficient crossing from the S_1 state to the ground state (S_0) is possible in the base-stacked case or changes the energy gap between the fluorescent $\pi\pi^*$ S_1 state and the S_2 state, effectively a dark state. If the energies of the S_1 and S_2 states were closer in the base-stacked case than in the case of 2-aminopurine alone, then base stacking could facilitate internal conversion to the nonfluorescent S_2 state (note that the initially formed excited state has ~6 kcal/mol of excess vibrational energy). The oscillator strength for the transition between the ground state and the S_2 state is extremely low in all cases, and once in the S_2 state, the molecule will most likely return to the ground state via a nonradiative route. Figure 6 shows the relative energies of the first 10 vertical excited states for 2-aminopurine alone, 2-aminopurine stacked between the different nucleobases, and 2-aminopurine hydrogen-bonded to thymine. The energies have been adjusted so that the first excited state (the fluorescent $\pi\pi^*$ state) is taken to be zero in all cases. Figure 6 clearly shows that while no reduction in the energy gap between the first $\pi\pi^*$ and nπ^* states is observed, the splitting between S_1 and S_2 (a state of Rydberg character) does decrease substantially when 2-aminopurine is base-stacked with guanine, and to a lesser amount when 2-aminopurine is base-stacked with cytosine, indicating that an increased rate of internal conversion from S_1 to S_2 is a possible explanation for an increased nonradiative rate in the case of 2-aminopurine stacked with guanine.

In the case of pyrrolocytosine, the CIS method again predicts a decrease in the oscillator strength for the fluorescence transition when pyrrolocytosine is base-stacked with guanine. The decrease in oscillator strength would, as described above, lead to a decrease in the fluorescence quantum yield when pyrrolocytosine was involved in a base-stacked environment, in agreement with the available experimental data. As no experimental determination of the excited fluorescent-state lifetime of pyrrolocytosine or structures containing pyrrolocytosine has been published, we cannot comment upon whether the observed fluorescence quenching is simply caused by a reduction in the oscillator strength for the fluorescent transition or whether an increase in the nonradiative rate also occurs with base stacking. It is interesting to note that a larger gap between the first and second excited states is found when the energy manifolds of free pyrrolocytosine are compared to that of structures in which pyrrolocytosine is sandwiched between two guanine moieties, indicating that if fast S_1 to S_2 crossing causes reduced fluorescence for systems in which 2-aminopurine is base-stacked with guanine, the same should not be true for structures containing pyrrolocytosine.

[3] The fluorescence quantum yield for dinucleotides containing 2-aminopurine were estimated in refs *3* and *12* by obtaining the ratio of the fluorescence signal obtained for the dinucleotide to that of free 2-aminoupruine in solution. As the absorption coefficient for the dinucleotide is not the same as that of free 2-aminopurine, the quantum yields can be taken as lower limits, having said that the value reported for $^{5'}$2APG$^{3'}$ was 0.065 (*3*) and 0.04 (*12*) relative to free 2-aminopurine, i.e., a 15−25-fold reduction.

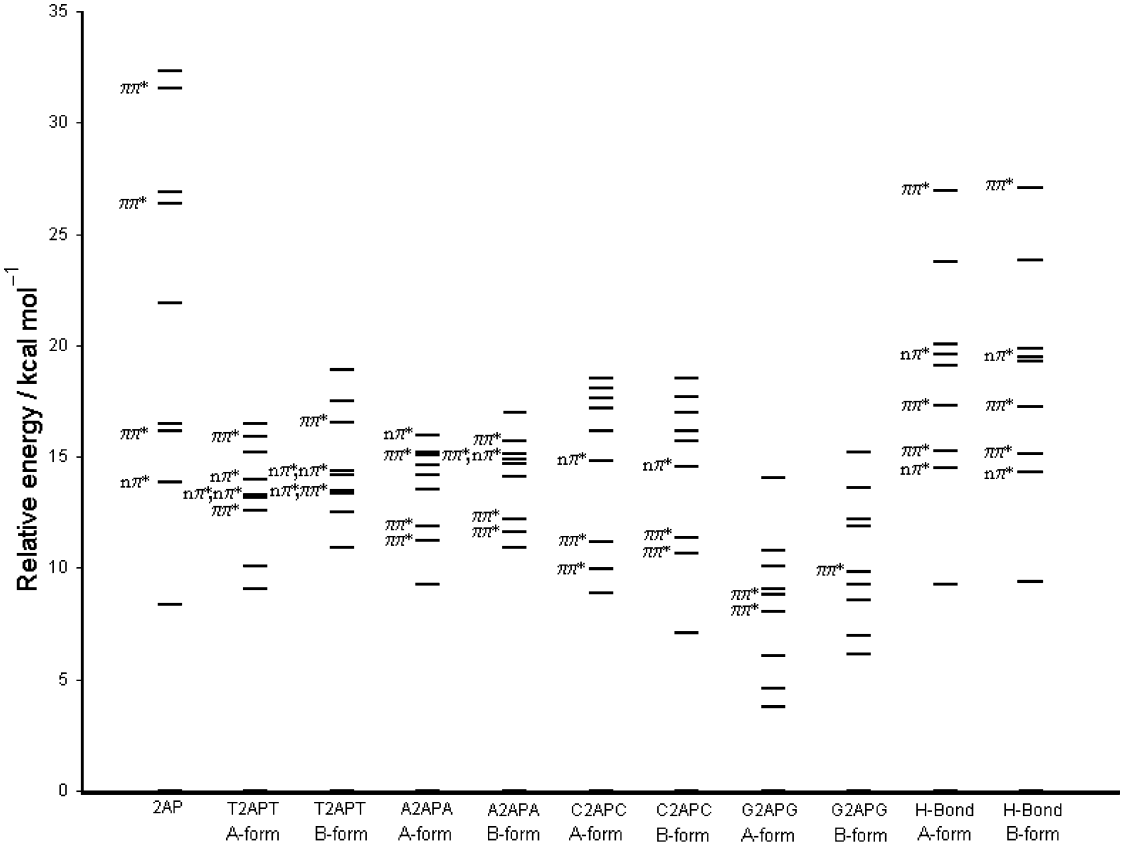

FIGURE 6: Manifold of excited states for the various complexes studied in this work. The energy of the first excited state (the fluorescent $\pi\pi^*$ state in all cases) has been taken to be zero in each case. All energies were calculated at the CIS/6-31+G(d,p) level and have been scaled by a constant factor of 0.72. If no assignment is given, then the state is of Rydberg or $\pi\sigma^*$ character.

In conclusion, we have studied the vertical transition energies and oscillator strengths for transitions between the ground state and excited states of 2-aminopurine, complexes in which 2-aminopurine is hydrogen-bonded to thymine, and structures representative of 2-aminopurine and the other nucleobases (thymine, cytosine, guanine, and adenine) as they would be stacked in A- and B-form DNA. The excited-state properties of the complexes were studied using the CIS method as problems with low-lying charge-transfer states make the TDB3LYP method unsuitable and more exact ab initio methods cannot at present be applied to such large systems. Using a simplified picture, where the geometry of the excited-state complex was taken to involve changes in the geometry of the 2-aminopurine base and not the relative positions of the bases in the complex or the geometries of the other nucleobases, the results suggest that hydrogen bonding does not have a major influence on the fluorescence properties of 2-aminopurine; indeed, the fluorescence transition predicted for the complex is just that of 2-aminopurine alone. In contrast, base stacking is predicted to dramatically alter the nature of the fluorescence (and absorption) transition, in that the orbitals involved in the fluorescence transition are no longer centered purely on 2-aminopurine but have components on the other bases as well. The magnitude of the oscillator strength associated with the fluorescence transition decreases by up to 53%, thus reducing the expected fluorescence quantum yield. The effect is most pronounced when 2-aminopurine is stacked with a purine base rather than a pyrimidine base, indicating an interaction between the π orbitals, purines having a more extended π system than pyrimidine bases. This reduction in fluorescence quantum yield should, however, be accompanied by a slight increase in the excited-state lifetime, and this has not been observed experimentally, indicating that base stacking must not only change the oscillator strength for the fluorescence transition but also open up other, nonradiative pathways. The nature of these nonradiative pathways is as yet unknown and could include charge-transfer processes (our results show that only charge transfer does not occur initially upon excitation of 2-aminopurine). Examination of the spacing between the various excited states of the base-stacked structures reveals that base stacking significantly alters the nature of the states and the spacing between them. In the case where 2-aminopurine is sandwiched between two guanine moieties, a significant decrease in the spacing between S_1 and S_2 is apparent, opening up the possibility of an increased rate of internal conversion from S_1 to the dark S_2 state and hence quenching of the fluorescence.

In the case of another nucleobase, pyrrolocytosine, a similar decrease in oscillator strength with the degree of base stacking has been observed, but in contrast to structures containing 2-aminopurine, there is no evidence that the π orbitals involved spread over more than one base in the case of pyrrolocytosine and the gap between the S_1 and S_2 states increases slightly when pyrrolocytosine is base-stacked with guanine. The fluorescence of both pyrrolocytosine and 2-aminopurine is significantly quenched in helical DNA, but there is insufficient experimental evidence available to date to judge whether the nature of the quenching in the case of

pyrrolocytosine is likely to be the same as that for 2-aminopurine.

ACKNOWLEDGMENT

We thank the EPSRC, Computational Chemistry Working Party, for the award of computer time on the Columbus cluster.

SUPPORTING INFORMATION AVAILABLE

Cartesian coordinates for all structures for which novel results are presented in this papers. This material is available free of charge via the Internet at http://pubs.acs.org.

REFERENCES

1. Rist, M. J., and Marino, J. P. (2002) Fluorescent nucleotide base analogs as probes of nucleic acid structure, dynamics and interactions, *Curr. Org. Chem. 6*, 775−793.
2. Martin, C. T., Újvári, A., and Liu, C. (2003) Evaluation of fluorescence spectroscopy methods for mapping melted regions of DNA along the transcription pathway, *Methods Enzymol. 371*, 13−33.
3. Reynisson, J., and Steenken, S. (2005) One-electron reduction of 2-aminopurine in the aqueous phase. A DFT and pulse radiolysis study, *Phys. Chem. Chem. Phys. 7*, 659−665.
4. Wan, C., Xia, T., Becker, H.-C., and Zewail, A. H. (2005) Ultrafast unequilibrated charge transfer: A new channel in the quenching of fluorescent biological probes, *Chem. Phys. Lett. 412*, 158−163.
5. Somsen, O. J. G., van Hoek, A., and van Amerongen, H. (2005) Fluorescence quenching of 2-aminopurine in dinucleotides, *Chem. Phys. Lett. 402*, 61−65.
6. Jean, J. M., and Hall, K. B. (2004) Stacking−unstacking dynamics of oligodeoxynucleotide trimers, *Biochemistry 43*, 10277−10284.
7. O'Neill, M. A. T., Becker, H.-C., Wan, C., Barton, J. K., and Zewail, A. H. (2003) Ultrafast dynamics in DNA-mediated electron transfer: Base gating and the role of temperature, *Angew. Chem., Int. Ed. 42*, 5896−5900.
8. Fiebig, T., Wan, C., and Zewail, A. H. (2002) Femtosecond charge-transfer dynamics of a modified DNA base: 2-Aminopurine in complexes with nucleotides, *ChemPhysChem 3*, 781−788.
9. Larsen, O. F. A., van Stokkum, I. H. M., Gobets, B., van Grondelle, R., and van Amerongen, H. (2001) Probing the structure and dynamics of a DNA hairpin by ultrafast quenching and fluorescence depolarization, *Biophys. J. 81*, 1115−1126.
10. Wan, C., Fiebig, T., Schieman, O., Barton, J. K., and Zewail, A. H. (2000) Femtosecond direct observation of charge transfer between bases in DNA, *Proc. Natl. Acad. Sci. U.S.A. 97*, 14052−14055.
11. Kelley, S. O., and Barton, J. K. (1999) Electron transfer between bases in double helical DNA, *Science 283*, 375.
12. Larsen, O. F. A., van Stokkum, I. H. M., de Weerd, F. L., Vengris, M., Aravindakumar, C. T., van Grondelle, R., Geacintov, N. E., and van Amerongen, H. (2004) Ultrafast transient-absorption and steady-state fluorescence measurements on 2-aminopurine substituted dinucleotides and 2-aminopurine substituted DNA duplexes, *Phys. Chem. Chem. Phys. 6*, 154−160.
13. Rachofsky, E. L., Seibert, E., Stivers, J. T., Osman, R., and Ross, J. B. (2001) Conformation and dynamics of abasic sites in DNA investigated by time-resolved fluorescence of 2-aminopurine, *Biochemistry 40*, 957−967.
14. Guest, C. R., Hochstrasser, R. A., Sowers, L. C., and Millar, D. P. (1991) Dynamics of mismatched base-pairs in DNA, *Biochemistry 30*, 3271−3279.
15. Nordlund, T. M., Andersson, T. M., Nilsson, L., Rigler, R., Gräslund, A., and McLaughlin, L. W. (1989) Structure and dynamics of a fluorescent DNA oligomer containing the EcoRI recognition sequence: Fluorescence, molecular-dynamics, and NMR-studies, *Biochemistry 28*, 9095−9103.
16. Jean, J. M., and Hall, K. B. (2002) 2-Aminopurine electronic structure and fluorescence properties in DNA, *Biochemistry 41*, 13152−13161.
17. Jean, J. M., and Hall, K. B. (2001) 2-Aminopurine fluorescence quenching and lifetimes: Role of base stacking, *Proc. Natl. Acad. Sci. U.S.A. 98*, 37−41.
18. Becke, A. D. (1993) Density-functional thermochemistry. 3. The role of exact exchange, *J. Chem. Phys. 98*, 5648−5652.
19. Lee, C. T., Yang, W. T., and Parr, R. G. (1988) Development of the Colle-Salvetti correlation-energy formula into a functional of the electron-density, *Phys. Rev. B 37*, 785−789.
20. Foresman, J. B., Head-Gordon, M., Pople, J. A., and Frisch, M. J. (1992) Toward a systematic molecular-orbital theory for excited-states, *J. Phys. Chem. 96*, 135−149.
21. Berry, D. A., Jung, K. Y., Wise, D. S., Sercel, A. D., Pearson, W. H., Mackie, H., Randolph, J. B., and Somers, R. L. (2004) Pyrrolo-dC and pyrrolo-C: Fluorescent analogs of cytidine and 2′-deoxycytidine for the study of oligonucleotides, *Tetrahedron Lett. 45*, 2457−2461.
22. Tinsley, R. A., and Walter, N. G. (2006) Pyrrolo-C as a fluorescent probe for monitoring RNA secondary structure formation, *RNA* (10.1261/rna.2165806).
23. *Spartan02* (2002) Wavefunction Inc., Irvine, CA.
24. Thompson, K. C., and Miyake, N. (2005) Properties of a new fluorescent cytosine analogue, pyrrolocytosine, *J. Phys. Chem. B 109*, 6012−6019.
25. Sándorfy, C. (1999) in *The role of Rydberg states in spectroscopy and photochemistry* (Sándorfy, C., Ed.) Kluwer Academic Publishers, Dordrecht, The Netherlands.
26. Frisch, M. J., Trucks, G. W., Schlegel, H. B., Scuseria, G. E., Robb, M. A., Cheeseman, J. R., Montgomery, J. A., Jr., Vreven, T., Kudin, K. N., Burant, J. C., Millam, J. M., Iyengar, S. S., Tomasi, J. J., Barone, V., Mennucci, B., Cossi, M., Scalmani, G., Rega, N., Petersson, G. A., Nakatsuji, H., Hada, M., Ehara, M., Toyota, K., Fukuda, R., Hasegawa, J., Ishida, M., Nakajima, T., Honda, Y., Kitao, O., Nakai, H., Klene, M., Li, X., Knox, J. E., Hratchian, H. P., Cross, J. B., Adamo, C., Jaramillo, J., Gomperts, R., Stratmann, R. E., Yazyev, O., Austin, A. J., Cammi, R., Pomelli, C., Ochterski, J. W., Ayala, P. Y., Morokuma, K., Voth, G. A., Salvador, P., Dannenberg, J. J., Zakrzewski, V. G., Dapprich, S., Daniels, A. D., Strain, M. C., Farkas, O., Malick, D. K., Rabuck, A. D., Raghavachari, K., Foresman, J. B., Ortiz, J. V., Cui, Q., Baboul, A. G., Clifford, S., Cioslowski, J., Stefanov, B. B., Liu, G., Liashenko, A., Piskorz, P., Komaromi, I., Martin, R. L., Fox, D. J., Keith, T., Al-Laham, M. A., Peng, C. Y., Nanayakkara, A., Challacombe, M., Gill, P. M. W., Johnson, B., Chen, W., Wong, M. W., Gonzalez, C., and Pople, J. A. (2003) *Gaussian 03*, revision B.04, Gaussian, Inc., Pittsburgh, PA.
27. Flükiger, P., Lüthi, H. P., Portmann, S., and Weber, J. (2000) *MOLEKEL 4.0*, Swiss Center for Scientific Computing, Manno, Switzerland.
28. Zhurko, G. A. (2005) *Chemcraft*, version 1.5, http://www.chemcraftprog.com.
29. Broo, A., and Holmén, A. (1997) Calculations and characterization of the electronic spectra of DNA bases based on ab initio MP2 geometries of different tautomeric forms, *J. Phys. Chem. A 101*, 3589−3600.
30. Rachofsky, E. L., Ross, J. B. A., Krauss, M., and Osman, R. (2001) CASSCF investigation of electronic excited states of 2-aminopurine, *J. Phys. Chem. A 105*, 190−197.
31. Dreuw, A., and Head-Gordon, M. (2005) Single-reference ab initio methods for the calculation of excited states of large molecules, *Chem. Rev. 105*, 4009−4037.
32. Kobayashi, R., and Amos, R. D. (2006) The application of CAM-B3LYP to the charge-transfer band problem of the zincbacteriochlorin-bacteriochlorin complex, *Chem. Phys. Lett. 420*, 106−109.
33. Cho, H. S., Jeong, D. H., Yoon, M.-C., Kim, Y. H., Kim, Y.-R., Kim, D., Jeoung, S. C., Kim, S. K., Aratani, N., Shinmori, H., and Osuka, A. (2001) Excited-State Energy Transfer Processes in Phenylene- and Biphenylene-Linked and Directly-Linked Zinc(II) and Free-Base Hybrid Diporphyrins, *J. Phys. Chem. A 105*, 4200−4210.
34. Russo, N., Toscano, M., and Grand, A. (2000) Theoretical determination of electron affinity and ionization potential of DNA and RNA bases, *J. Comput. Chem. 21*, 1243−1250.
35. Sugiyama, H., and Saito, I. (1996) Theoretical studies of GG-specific photocleavage of DNA via electron transfer: significant lowering of ionization potential and 5′-localization of HOMO of

stacked GG bases in B-from DNA, *J. Am. Chem. Soc. 118*, 7063−7068.
36. Rachofsky, E. L., Osman, R., and Ross, J. B. A. (2001) Probing structure and dynamics of DNA with 2-aminopurine: Effects of local environment on fluorescence, *Biochemistry 40*, 946−956.
37. Strickler, S. J., and Berg, R. A., (1962) Relationship between absorption intensity and fluorescence lifetime of molecules, *J. Chem. Phys. 37*, 814−822.
38. Atkins, P. W., and de Paula, J. (2001) *Physical Chemistry*, 7th ed., Oxford University Press, New York.
39. Ward, D. C., Reich, E., and Stryer, L. (1969) Fluorescence studies of nucleotides and polynucleotides, *J. Biol. Chem*. *244*, 1228−1237.
40. Holmén, A., Nordén, B., and Albinsson, B. (1997) Electronic transition moments of 2-aminopurine, *J. Am. Chem. Soc. 119*, 3114−3121.
41. Neely, R. K., Magennis, S. W., Dryden, D. T. F., and Jones, A. C. (2004) Evidence of tautomerism in 2-aminopurine from fluorescence lifetime measurements, *J. Phys. Chem. B 108*, 17606−17610.
42. Santhosh, C., and Mishra, P. C. (1991) Electronic spectra of 2-aminopurine and 2,6-diaminopurine: Phototautomerism and fluorescence reabsorption, *Spectrochim. Acta 47A*, 1685−1693.

BI060479T